Assimilation of Satellite-Observed Snow Albedo in a Land Surface Model

M. JAHANZEB MALIK

Faculty of Geo-Information Science and Earth Observation (ITC), University of Twente, Enschede, Netherlands, and Pakistan Space and Upper Atmosphere Research Commission, Karachi, Pakistan

ROGIER VAN DER VELDE, ZOLTAN VEKERDY, AND ZHONGBO SU

Faculty of Geo-Information Science and Earth Observation (ITC), University of Twente, Enschede, Netherlands

(Manuscript received 30 September 2011, in final form 2 December 2011)

ABSTRACT

This study assesses the impact of assimilating satellite-observed snow albedo on the Noah land surface model (LSM)-simulated fluxes and snow properties. A direct insertion technique is developed to assimilate snow albedo into Noah and is applied to three intensive study areas in North Park (Colorado) that are part of the 2002/03 Cold Land Processes Field Experiment (CLPX). The assimilated snow albedo products are 1) the standard Moderate Resolution Imaging Spectrometer (MODIS) product (MOD10A1) and 2) retrievals from MODIS observations with the recently developed Pattern-Based Semiempirical (PASS) approach. The performance of the Noah simulations, with and without assimilation, is evaluated using the in situ measurements of snow albedo, upward shortwave radiation, and snow depth. The results show that simulations with albedo assimilation agree better with the measurements. However, because of the limited impact of snow albedo updates after subsequent snowfall, the mean (or seasonal) error statistics decrease significantly for only two of the three CLPX sites. Though the simulated snow depth and duration for the snow season benefit from the assimilation, the greatest improvements are found in the simulated upward shortwave radiation, with root mean squared errors reduced by about 30%. As such, this study demonstrates that assimilation of satellite-observed snow albedo can improve LSM simulations, which may positively affect the representation of hydrological and surface energy budget processes in runoff and numerical weather prediction models.

1. Introduction

The albedo of snow affects the shortwave (SW; spectral range from 0.3 to 2.5 μm) radiative flux at the land–atmosphere interface and is, therefore, important for calculation of surface energy as well as mass (water) budgets. During snow cover periods, however, the albedo changes because of snow metamorphic processes [e.g., melt–freeze cycles, wind redistribution, sublimation, and vapor diffusion (DeWalle and Rango 2008)]. It is generally understood that the albedo decreases as the snow grain size increases (Wiscombe and Warren 1980). Livneh et al. (2010) recently included the effect of this albedo decay within the cold season processes component of the Noah land surface model (LSM; Ek et al. 2003). The authors incorporated an exponential decay as a function of snow age. Nevertheless, uncertainties in the snow albedo simulations still exist because of the fact that the rate of snow albedo decay depends on the dynamics of atmosphere near the surface, which is ignored. Moreover, LSM simulations are also subject to other sources of uncertainties, such as forcings, parameterization, initialization, and spatial discretization of the land surface.

On the other hand, the snow albedo can be observed remotely with satellite sensors. Several approaches exist for snow albedo retrieval from remote sensing observations. These include lookup table approaches (Painter et al. 2009; Stamnes et al. 2007), empirical approaches based on anisotropic reflectance function (ARF), (Klein and Stroeve 2002; Liang et al. 2005), and (semi) analytical approaches (Kokhanovsky and Zege 2004; Lyapustin et al. 2009; Tedesco and Kokhanovsky 2007) based on Lambertian reflectance for the snow albedo retrieval. Recently, Malik

Corresponding author address: M. Jahanzeb Malik, Faculty of Geo-Information Science and Earth Observation (ITC), University of Twente, Hengelosestraat 99, 7500 AE Enschede, The Netherlands.
E-mail: malik14406@itc.nl

DOI: 10.1175/JHM-D-11-0125.1

et al. (2011) presented a Pattern-Based Semiempirical (PASS) approach, which exploits triangular variability pattern of albedo and reflectance formed because of varying sun-sensor geometry to retrieve snow albedo. The authors obtained with this method a 50% better agreement with in situ measurements as compared to the Moderate Resolution Imaging Spectroradiometer (MODIS) product (i.e., MOD10A1 daily snow albedo estimates; Klein and Stroeve 2002).

Integration of these satellite-based products within LSMs, such as Noah, can assist in further reducing the uncertainties discussed above. Several successful examples can be found on the assimilation of snow variables. For example, Rodell and Houser (2004) adjusted snow water equivalent (SWE) using MODIS fractional snow coverage (FSC) information when and where the model and MODIS observation differs. Similarly, Andreadis and Lettenmaier (2006) and Zaitchik and Rodell (2009) updated SWE from MODIS FSC estimates using an ensemble Kalman filter (EnKF) and rule-based direct insertion (DI), respectively. However, the usage of satellite-based snow albedo products has so far not yet been explored for assimilation.

The objective of the study is to assess the impact of assimilating snow albedo estimates on the fluxes and snow properties simulated by the Noah LSM. We focus on reducing the uncertainty in Noah simulations by assimilating the snow albedo via the DI technique. Because DI assumes that the observations ingested into the modeling system are error free, three snow albedo products with different inherent uncertainties have been selected for assimilation—namely, the ground measurements and the MODIS-based snow albedo products from Malik et al. (2011) and the standard MOD10A1. As such, the assumption of error-free observations is quantified by updating Noah with observations of different inherent uncertainties.

Physics describing the snow processes in the LSM have recently been improved (Barlage et al. 2010; Livneh et al. 2010; Wang et al. 2010). Hence, the focus is on the assessment of the assimilation impact rather than on improving the model physics. The 2002/03 winter season measured during the Cold Land Processes Field Experiment (CLPX) is selected as a test bed because it includes remote sensing observations as well as the in situ measurements needed to force and to validate Noah. The structure of this paper is as follows: section 2 describes the study area and the ground measurements. Section 3 describes the satellite-based snow albedo products used for assimilation. Section 4 presents the relevant cold season processes included in the Noah LSM and the control (or open loop) simulations (i.e., without snow albedo updates). In section 5, the data assimilation procedure is described and the results are presented. Finally, some concluding remarks are given in section 6.

2. CLPX

a. Study area

During the CLPX 2002/03 winter season, data were collected at three mesocell study areas (MSA) in Colorado, each covering an area of about 25×25 km^2. In situ measurements within the MSAs were collected at three 1-km^2 intensive study areas (ISA). We selected for our study the sites with low-topographic relief and without forest to minimize the uncertainties in satellite-observed snow albedo. The utilized ISAs are Illinois River [North Park, Illinois River (NI); 40.6954°N, 106.2545°W; World Geodetic System 1984 (WGS 84) ellipsoid model], Michigan River [North Park, Michigan River (NM); 40.6450°N, 106.1809°W; WGS 84], and Potter Creek [North Park, Potter Creek (NP); 40.6677°N, 106.3232°W; WGS 84). All the sites are located within the North Park MSA.

The North Park MSA has very low relief and grassland dominates the land cover. The MSA has a mean elevation of 2499 m and the predominant soil texture is sandy loam. Snowpacks at North Park can be classified as prairie and tundra covers (Sturm et al. 1995), which are representative for about 53% of seasonally snow-covered areas globally. The soils are typically frozen during the winter season because of the shallow and windswept snow cover. More information about the North Park MSA and its ISAs can be found at http://www.nohrsc.nws.gov/~cline/clpx.html.

b. Ground measurements

The field measurements, needed to run (force and initialize) as well as to validate Noah, were collected at the CLPX meteorological towers in the center of the ISAs named: NI, NM, and NP. Soil moisture and soil and skin temperature measurements are used for the model initialization. The CLPX wind speed, wind direction, air temperature, relative humidity, atmospheric pressure, and short- and longwave downward radiation are used as forcings. The atmospheric variables were recorded at a 10-min interval 2 m above the ground surface in the MSA (Elder and Goodbody 2004; Elder et al. 2009). Precipitation inputs are obtained from the North American Land Data Assimilation System version 2 (NLDAS-2; Ek et al. 2011; Xia et al. 2011), which is an hourly merged gauge-radar product at $\frac{1}{8}°$ (or 12.5 km) spatial resolution.

The meteorological towers were also equipped with an acoustic sounder for measuring snow depths with an estimated accuracy of ± 1.0 cm (Elder et al. 2009). These snow depths, the upward shortwave radiation, and the albedo derived from the measurements made by net radiometers are used to evaluate Noah's performance with and without the snow albedo assimilation. Details of the instruments

TABLE 1. List of instruments and respective measurements taken during CLPX that are used in this study.

Variable	Instruments	Accuracy
Atmospheric pressure	Vaisala PTB101B pressure transmitter	±6 hPa
Air temperature	Vaisala HMP45C temperature and relative humidity probe	±0.5°C
Relative humidity	Vaisala HMP45C temperature and relative humidity probe	±3%
Wind speed and direction	R. M. Young 05103 wind monitor	±2% and ±5°
SW downward and upward radiation	Kipp and Zonen CNR1 net radiometer	±10%
Acoustic depth sounder	Judd ultrasonic depth sensor	±1 cm
Soil moisture and temperature	Stevens Vitel Hydra Probe	±0.03 and 0.6°C
Surface temperature	Apogee IRTS-P5 infrared thermocouple	±0.4°C

employed during the CLPX to collect the measurements utilized for this study are provided in Table 1.

3. Satellite-observed snow albedo products

The two satellite-based snow albedo products utilized to update Noah are retrieved from MODIS observations, which is a key instrument on board the National Aeronautics and Space Administration (NASA)'s *Terra* platform. The first is the operational level-3 product (MOD10A1) and the other one is derived from the MODIS level-1B shortwave infrared (SWIR) radiance product (MOD02HKM) using the algorithm developed by Malik et al. (2011). Both albedo products are available at a 500-m spatial resolution and the retrieval algorithms are briefly described below.

The MOD10A1 level-3 product provides estimates of fractional snow cover and albedo via application of the empirical approaches developed by Salomonson and Appel (2004) and Klein and Stroeve (2002), respectively. The empirical approach of Klein and Stroeve (2002) computes via a linear combination of the seven 500-m resolution MODIS bands the broadband snow albedo (i.e., 0.3–2.5 μm), as follows:

$$\alpha_{\text{snow}} = \sum_{i=1}^{7} c_i a_i, \tag{1}$$

where α_{snow} is the broadband snow albedo, i is the MODIS band number, a_i is the corrected spectral albedo of the ith MODIS band for the anisotropic effects, and c_i are experimentally determined coefficients.

The MODIS snow albedo product by Malik et al. (2011) is computed as a function of the SWIR (1.230–1.250 μm, band 5) directional reflectance (units sr^{-1}), derived from the MOD02HKM radiance [units W $(\text{m}^2\ \mu\text{m sr})^{-1}$]. The developed PASS approach retrieves the spectral snow albedo from the observed reflectance, while accounting for the directional effects due to varying sun-sensor geometry represented by a right triangular pattern. The base (b) of this triangle is defined as a function of the solar zenith and the height (h) is given by the scattering angle, as follows:

$$b = 0.29 - \int_0^{\theta'_o} [(1.4 \times 10^{-006}\theta_o^2) + (3.6 \times 10^{-006}\theta_o) + 0.000\,61]\, d\theta_o, \quad \text{and} \tag{2}$$

$$h = 0.43 - \int_{40}^{\theta'_{\text{sca}}} [(-1.9 \times 10^{-008}\theta_{\text{sca}}^3) + (7.9 \times 10^{-006}\theta_{\text{sca}}^2) - (0.0011\theta_{\text{sca}}) + 0.05]\, d\theta_{\text{sca}}, \tag{3}$$

where θ_o and θ_{sca} are incident and scattering angles, respectively, and θ'_o and θ'_{sca} are incident and scattering angles used for the radiance measurement. The b and h in combination with the directional reflectance provide the spectral albedo (a_{sp}), which is converted into the broadband snow albedo as follows:

$$\alpha_{\text{nir}} = 1.1a_{\text{sp}}^3 - 1.1a_{\text{sp}}^2 + 0.86a_{\text{sp}} + 0.098, \quad \text{and} \tag{4}$$

$$\alpha_{\text{snow}} = \alpha_{\text{vis}} f_{\text{vis}} + \alpha_{\text{nir}}(1 - f_{\text{vis}}), \tag{5}$$

where α_{nir} is near-infrared albedo, α_{vis} is visible albedo, f_{vis} is the visible light fraction of shortwave downwelling radiation, and α_{snow} is broadband snow albedo.

Stroeve et al. (2006) evaluated the *Terra* MOD10A1 product with in situ measurements collected over Greenland and reported an overall root-mean-square error (RMSE) of 0.067 and correlation coefficient (r) of 0.79. Malik et al. (2011) obtained similar results (i.e., RMSE of 0.064 and $r = 0.6$), with MOD10A1 over the North Park CLPX sites and the Namco Lake on the Tibetan Plateau.

TABLE 2. Initial states and parameters used for the NI site Noah simulations. Italic parameters are derived from NLDAS and others are obtained from the CLPX measurements.

Noah parameters and initial conditions	Assigned values			
Start date (yyyymmddhhmm)	200210260600			
End date (yyyymmddhhmm)	200303152350			
Latitude (decimal degrees)	40.6954			
Longitude (decimal degrees)	−106.2545			
Forcing time step (s)	600			
Noah LSM time step (s)	600			
Soil layer thickness (m)	0.1	0.2	0.4	1.0
Soil temperature (K)	272	276	277	278
Soil moisture ($m^3\ m^{-3}$)	0.109	0.227	0.0054	0.0054
Soil liquid ($m^3\ m^{-3}$)	0.109	0.227	0.0054	0.0054
Skin temperature (K)	269.77			
Snow depth (m)	0			
Snow equivalent (m)	0			
Deep soil temperature (K)	278			
Land use dataset	U.S. Geological Survey (USGS)			
Soil type index	3 (i.e., sandy loam)			
Vegetation type index	9 (i.e., mixed shrubland–grassland)			
Slope type index	1			
Max snow albedo	0.85			
Air temperature level (m)	2			
Wind level (m)	2			
Green vegetation min	0.01			
Green vegetation max	0.5			

The error statistics reported in Malik et al. (2011) for the PASS approach are, with a RMSE = 0.03 and a $r = 0.8$ for the CLPX's North Park and Tibetan Plateau sites, better than the MOD10A1 product.

4. Noah snow process simulations

a. Model physics

Noah (Ek et al. 2003; Mitchell et al. 2005) is a one-dimensional (i.e., fluxes are not exchanged across the model grid) process model that can operate either in coupled mode to a general circulation model (GCM) or an offline mode. Noah represents the snowpack as a single layer, for which the snow states are defined (i.e., albedo, density, depth, and water equivalent). In this study, we use the most recent public release (version 3.2), in which significant improvements have been made to the snow process physics (Barlage et al. 2010; Wang et al. 2010).

Most relevant for this study is the implementation of a time-varying snow albedo formulation reported in Livneh et al. (2010). The modified Noah simulates the snow albedo (α_{snow}) as the maximum broadband snow albedo ($\alpha_{\max}$) reduced by a time-dependent decay factor, which is reset to 1 on snowfall, as follows:

$$\alpha_{\text{snow}} = \alpha_{\max} A^{B^t}, \tag{6}$$

where A and B are constants defined differently for dry and wet snowpacks, and t is the time in days since the last snowfall. This formulation is adopted from Distributed Hydrology Soil Vegetation Model (DHSVM; Wigmosta et al. 1994) and has also been implemented in the Variable Infiltration Capacity (VIC) LSM (Cherkauer et al. 2003).

The exponential decay with time mimics the snow metamorphism, causing changes in the snow grain size and, as a result, the albedo. As the albedo is a variable in the surface energy budget, this modification alters the mass–water fluxes at the snow surface, affecting SWE simulations and, indirectly, snow depth. Also noteworthy is the improved snow-specific density formulation near the melting point, which impacts the snow depth simulations via its calculation as a ratio of the SWE over the snow-specific density.

b. Open-loop simulation

To provide a reference for the following sections, Noah is run without data assimilation for the NI ISA over the period of 26 October 2002–15 March 2003 using the atmospheric forcings described in section 2b. The initialization and parameterizations representative for the NI site are obtained from the CLPX measurements and NLDAS. Table 2 provides the adopted initial states and parameters.

Figure 1 shows the simulated and measured snow depth and albedo along with the NLDAS-2 precipitation. The simulations demonstrate that the model accumulates snow during winters, ablates snow at springtime, and, as such,

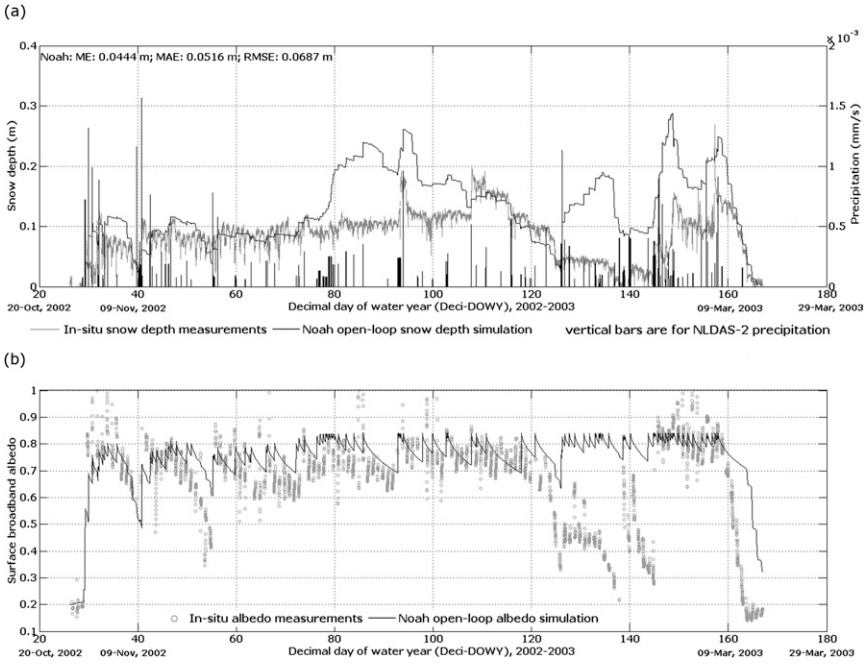

FIG. 1. In situ measured and Noah simulated for (a) snow depth and (b) snow albedo plotted over time along the with the NLDAS-2 precipitation. DOWY starts 1 Oct and ends 30 Sep.

simulates the duration of the snow season quite well. Nevertheless, some discrepancies can be noted between the simulated and measured snow depth and albedo. Especially in the period from 28 January to 17 February 2003 [decimal day of water year (Deci-DOWY) 120–140], the simulated snow depth and albedo deviate up to 0.15 m and 0.5, respectively. The albedo measurements are showing lower values than expected for any snow type (either fresh or old), but are still significantly higher than under snow-free conditions. This suggests that during this episode the snowpack was shallow and did not fully cover the surface, as is confirmed by the snow depth measurements (see Fig. 1a).

This observed discrepancy can be associated with the uncertain precipitation adopted from NLDAS-2. In fact, the NLDAS product is provided at a $1/8^{\circ}$ spatial resolution, whereas the snow measurements represent only a small area. As such, the NLDAS forcing may supply precipitation for a coarse grid cell, while on-site (NI) inputs were not received. Indeed, Fig. 1a shows an increase in the simulated snow depth and albedo in response to various snowfall events in that period, which is not in agreement with the measurements. Similarly, Pan et al. (2003) and Niu et al. (2011) highlighted the effects of uncertain precipitation input on snow process simulations. The period 28 January–17 February 2003 is, therefore, not further used for evaluation of the model performance.

Obviously, also outside the period 28 January–17 February 2003, differences are noted between the simulated and measured snow albedo. Figure 2 visualizes these deviations by plotting the simulations against the measurements. For this scatterplot, the Noah albedo is a daily average of values simulated between 1700 and 2100 UTC, which overlaps the MODIS overpass time

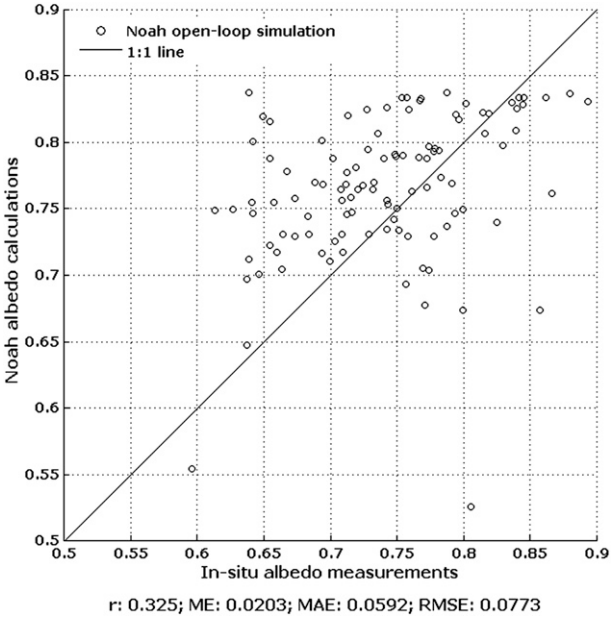

FIG. 2. Noah-simulated snow albedo plotted against in situ measurements. The points show average values of ±2 h at 1900 UTC of each day.

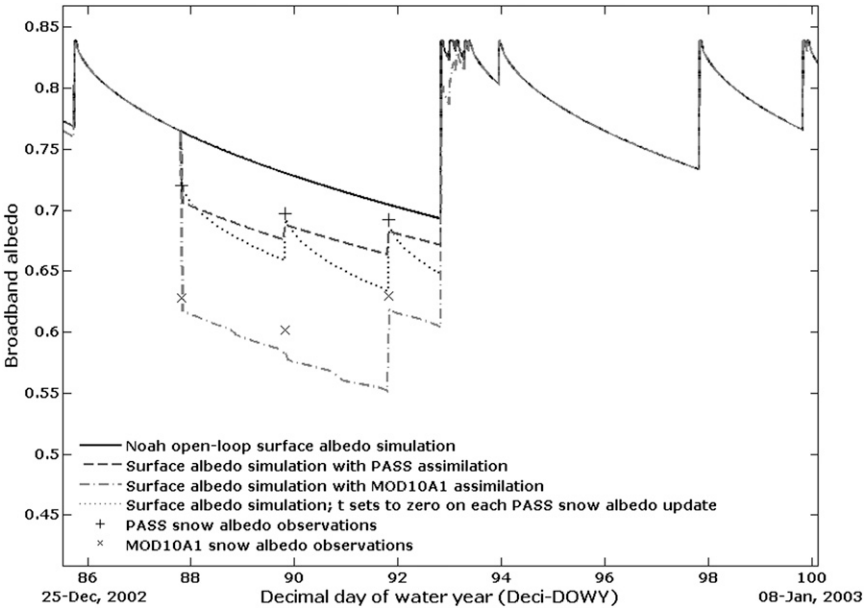

FIG. 3. Illustration of DI scheme for snow albedo assimilation. The black solid line shows the open-loop Noah simulation. The gray dashed and gray dashed–dotted lines are for the updated surface albedo simulations. Gray dashed line receives updates from the PASS approach (+ symbol) and gray dashed–dotted line obtains updates from MOD10A1 (× symbol). Gray dotted line represents the experiment where *t* sets to 0 at each albedo update (updates are from the PASS approach).

(1730–1855 UTC, or 1030–1155 local time). As such, the plot quantifies the Noah's performance in simulating the snow albedo near midday where most solar radiation exchange occurs. The error statistics show that Noah estimates albedo with a mean error (ME) of +0.0203, mean absolute error (MAE) of 0.0592, and RMSE of 0.0773. The statistics demonstrate that simulated snow albedo is on average quite close to the measurements (ME = +0.0203) and the deviations are on the same order of magnitude as reported for the MODIS snow albedo products (see section 3).

Although these error statistics indicate that Noah performs on average quite well, Fig. 2 also reveals some shortcomings. For example, the dynamic range of simulated snow albedo is about 40% smaller than the measured one. Moreover, the Noah tends to overestimate snow albedo. As a result, the Pearson's correlation coefficient (*r*) of about 0.3 is quite low.

5. Snow albedo assimilation

a. Assimilation approach

The approach employed for assimilation of the observed snow albedo with the Noah simulations is based upon a DI scheme. The assimilation consists of adjusting, without modifying the elapsed time since the last snowfall [*t* in Eq. (6)], the maximum broadband snow albedo

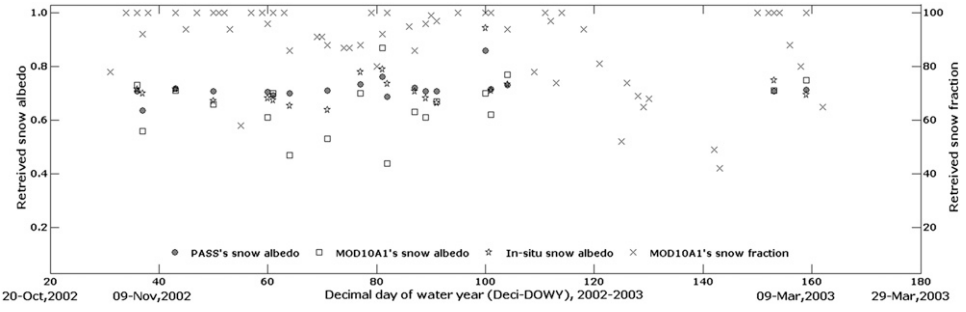

FIG. 4. MODIS snow fractional coverage, and three observed snow albedo products used for assimilation into Noah applied to the NI ISA.

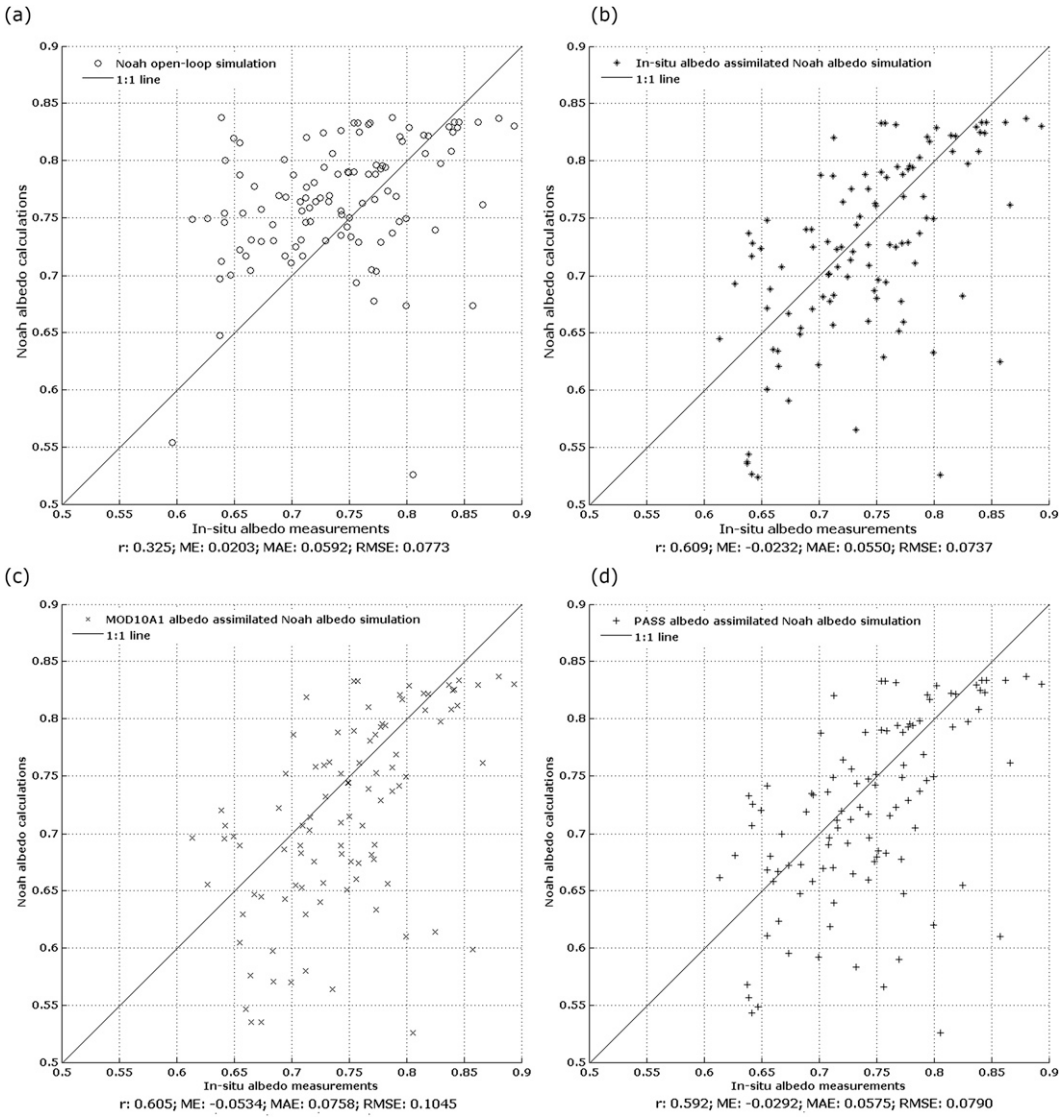

FIG. 5. Snow albedo scatterplots for the (a) open-loop and (b)–(d) updated Noah simulations compared to the in situ measurements. The points show average values for ±2 h at 1900 UTC of each day.

(α_{max}) such that the α_{snow} matches the observed albedo. This ensures that updating the snow albedo does not affect the decay rate and the integrity of the model physics is preserved—for example, decay of albedo at different rates for wet and dry snow, sharp albedo increase whenever snow falls, and the relationship between the decay rate and the snow age. The α_{max} is reset to its original value of 0.85 at the onset of each new snow event.

Figure 3 illustrates the procedure described above for the sequential assimilation of three observations. The MOD10A1 and MODIS snow albedo derived with the PASS approach are displayed as cross-marked and plus-marked points, respectively. The subsequent decay of the surface albedo is indicated by the dashed and dashed–dotted lines for PASS and MOD10A1 assimilated simulations, respectively. In addition, the dotted line shows the simulated snow albedo when also the t is reset to zero as a part of each update.

The open-loop Noah simulation (solid line) demonstrates the typical albedo decay after each snowfall. Assimilation of both MODIS products updates the Noah albedo in case observations are available without having a direct impact on the decay rate. However, a discrepancy between the observed snow albedo and the simulated surface albedo is noted. This is caused by a reduction in the fractional snow coverage associated with the decline in SWE (see Fig. 3) due to an increase in the radiation available for snowmelt. This also illustrates

TABLE 3. Error statistics of open-loop and updated snow albedo simulations for the NI site.

Site	Simulations	r	ME	MAE	RMSE
NI	Open loop	0.325	0.0203	0.0592	0.0773
NI	Updates: in situ	0.609	−0.0232	0.0550	0.0737
NI	Updates: MOD10A1	0.605	−0.0534	0.0758	0.1045
NI	Updates: PASS	0.592	−0.0292	0.0575	0.0790

the important role of snow albedo during the snow season for mass budget.

b. Updated simulations

Using the procedure described above, three different snow albedo observations, each with specific inherent uncertainties, are assimilated in the Noah model setup for the NI ISA. As mentioned previously, the albedo values are 1) derived from CLPX in situ measurements, 2) readily available MODIS products (MOD10A1), and 3) retrievals from MODIS observations using the PASS approach. The snow albedo is only assimilated when the MOD10A1 product indicates at least 90% snow coverage. This is needed to avoid the uncertainties associated with the subpixel heterogeneity imposed by the patchy snow cover typical for North Park.

A total of 19 MODIS observations fulfill the above criterion for the NI ISA and also for these dates alone the in situ albedo measurements are assimilated. Figure 4 shows the MODIS snow fractional coverage and the snow albedo values of the three products used for assimilation. Within this experimental setup, the in situ snow albedo is considered more accurate than the two satellite-based

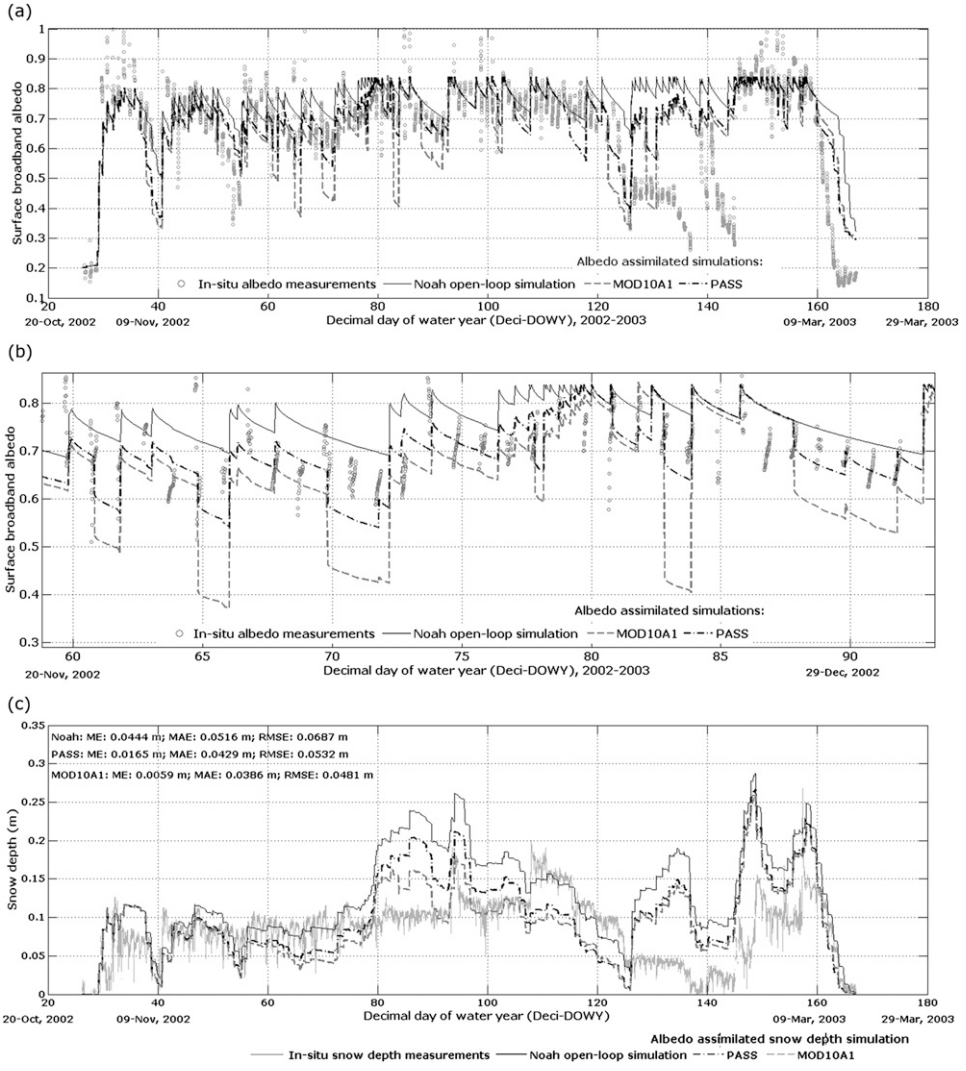

FIG. 6. In situ measurements and open-loop and updated Noah simulations for (a),(b) snow albedo and (c) snow depth. Panel (b) shows magnified view of (a). DOWY: 1 Oct–30 Sep.

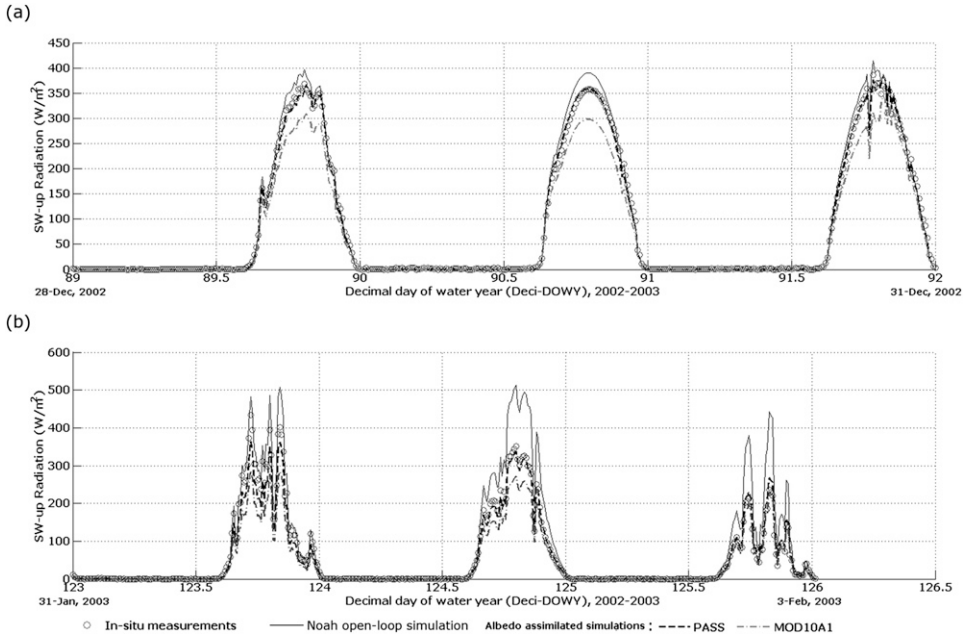

FIG. 7. In situ measurements, open-loop, and updated Noah simulations for SW upward radiations: (a) time lines from 28 to 31 Dec 2002 and (b) 31 Jan to 3 Feb 2003.

products. As such, the in situ albedo assimilation represents the maximum improvement that can be achieved with the selected number of observations.

Figure 5 compares the in situ and Noah-simulated albedo following from the open-loop run (Fig. 5a), assimilation of the in situ albedo (Fig. 5b), assimilation of the standard MODIS albedo (Fig. 5c), and assimilation of PASS approach MODIS albedo (Fig. 5d). These plots show four hourly averages centered on the MODIS overpass time for each day of the simulated snow season. The error statistics—ME, MAE, and RMSE shown in Table 3—indicate that assimilation does not significantly improve the albedo simulation as compared to the open-loop run for this snow season. However, the *r* increases from 0.325 for the open loop to about 0.600 for all three simulations with data assimilation. This suggests that assimilation improves the agreement between the daily in situ and simulated albedo variations. In this case, the reduction in the mean (or seasonal) error statistics is marginal mainly because the effect of the update extends only up to the next snowfall.

As noted above, the evaluation of the simulated against in situ snow albedo results in comparable values for *r* (~0.6) for the three Noah runs with data assimilation. The mean error statistics, however, do vary substantially. For example, the ME and RMSE are for assimilation of the MOD10A1 product is approximately 50% and 30% higher than for the assimilation of the snow albedo retrieved with the PASS approach. This is somewhat expected since we have previously shown that the PASS snow albedo is more accurate for the North Park MSA than the MOD10A1. Somewhat remarkable is the little difference in the error statistics observed between in situ and PASS updated simulations. This suggests that assimilation of snow albedo products with lesser uncertainty than the PASS product improves neither the *r* nor the mean error statistics significantly.

In addition, Fig. 6 evaluates the simulations of snow albedo (Figs. 6a,b) and snow depth (Fig. 6c) against the measured series. Figures 6a,b confirm that, shortly after updates, the simulated snow albedo values match the measurements better. The effect of this assimilation is, however, limited up to the next snow event. Hence, the simulation of the snow season duration is only slightly improved.

Also, the snow depth simulations (Fig. 6c) provide a better estimate of the measurements with use of the satellite snow albedo products. The dynamics of snow depth measurements are best represented in the simulations with the assimilation of MOD10A1 products. This is explained by the fact that Noah for this application overestimates the snow depth. As such, the strong negative bias (−0.0534) in the albedo simulation with MOD10A1 ingestion makes more energy available for melting, which results in a shallower snowpack. However, a firm conclusion about the "true" snow depth simulations is difficult to make as many aspects of the Noah snow depth are uncertain (e.g., atmospheric forcings, density, and liquid water fraction stored in the snowpack), as well as the measurements itself.

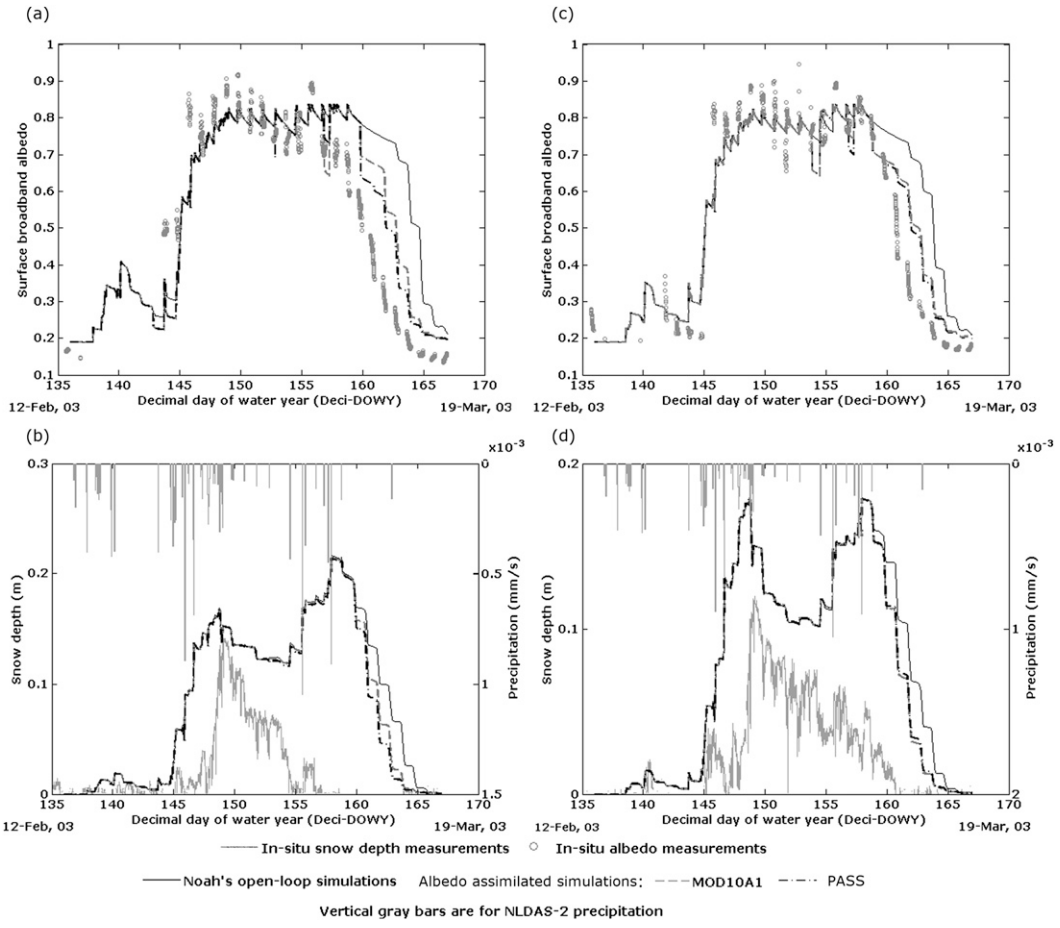

FIG. 8. Open-loop and updated Noah simulations for (a),(c) snow albedo and (b),(d) snow depth along with their in situ measurements for (a),(b) NM and (c),(d) NP sites.

Next to the simulation of snowpack properties, the snow albedo assimilation is also expected to impact the diurnal radiative fluxes. As an illustration, Figs. 7a,b show the measured and different simulated (''open loop'' and ''with assimilation'') upward shortwave radiations for two 3-day periods. The two plots demonstrate clearly that snow albedo assimilation improves the shortwave radiation simulation, whereby Noah's performance with PASS approach updates is better than with MOD10A1 updates. Over the complete simulation period, RMSE computed between the measurements and simulations reduces by 30% and 25% with assimilation of the PASS and MOD10A1 snow albedos, respectively. Based on these results, we conclude that the assimilation of snow albedo in Noah is particularly effective in improving radiative fluxes and, to a lesser extent, snow depth simulations.

c. *Simulations for NM and NP sites*

In support of the previous analysis, identical Noah simulations have been performed for the NM and NP sites in North Park. Similar to the NI simulation experiment, atmospheric forcings were adopted from the CLPX measurements collected at the respective sites supplemented with the NLDAS-2 precipitation product. Because of gaps in the measurement records, the simulation period is reduced from 12 February (i.e., Deci-DOWY is 135) to 19 March 2003 (i.e., Deci-DOWY is 170).

Figure 8 shows the open-loop as well as the updated snow albedo and depth simulations along with the in situ measurements. It is evident that for both the NM and NP sites, the snow albedo assimilation improves albedo simulations. In these applications the mean error statistics also reduce significantly—the RMSE decreases for the NM site from 0.212 to 0.148 and for the NP site from 0.163 to 0.123. This improvement is not reflected in the comparison of measured and simulated snow depths. It is, however, noted that the snow depth measurements at these two sites are low, which is inconsistent with the high albedo values. When ignoring the snow depth and only considering the albedo measurements, the

TABLE 4. Error statistics of open-loop and updated snow albedo simulations for NM and NP sites.

Site	Simulations	*r*	ME	MAE	RMSE
NM	Open loop	0.42	0.040	0.162	0.212
NM	Updates: MOD10A1	0.73	−0.001	0.125	0.159
NM	Updates: PASS	0.76	−0.009	0.117	0.148
NP	Open loop	0.52	0.029	0.114	0.163
NP	Updates: MOD10A1	0.84	−0.005	0.083	0.120
NP	Updates: PASS	0.85	−0.002	0.086	0.123

improvement obtained with assimilation also includes the duration of the snow season. Specifically, the snow cover depletion process is better represented within the updated simulations. Table 4 provides the error statistics of the albedo simulations for the different simulations.

For consistency with the NI experiments, Fig. 9 shows also upward shortwave radiation for the simulations performed for the NM and NP sites. Improvements as a result of snow albedo assimilation are also noticed here. The RMSE computed between measured and simulated upward shortwave radiation reduces for both test sites by about 35% when either the PASS approach or MOD10A1 are assimilated.

6. Conclusions and discussion

In the study, we investigate the potential benefit of assimilating satellite-observed snow albedo on fluxes and snow properties simulated by the Noah land surface model (LSM)—especially snow albedo, snow depth, and upward shortwave radiation. Two satellite-based snow albedo products are assimilated: 1) standard Moderate Resolution Imaging Spectrometer (MODIS) product (MOD10A1) and 2) the MODIS snow albedo retrieved with the Pattern-Based Semiempirical (PASS) approach. A technique based on direct insertion is developed for the assimilation and applied to 2002/03 North Park snow season observed at three sites during the Cold Land Process Field Experiment (CLPX).

The comparison with in situ measurements shows that, in general, assimilation improves the snow albedo simulations. A reduction in the mean (or seasonal) error statistics is, however, not evident for all three CLPX sites. This is attributed to the limited impact of snow albedo updates beyond the following snow event. Analyses also suggest that simulation of snow depth and the duration of snow season tend to improve with snow albedo assimilation. However, a firm conclusion on this aspect is not possible because of the many uncertainties involved in the modeling as well as measurement of these processes. The most noticeable improvements obtained with assimilation are in the simulation of the upward shortwave radiation. With both satellite-based albedo products the root-mean-square errors decrease by about 30%.

Therefore, we conclude that the assimilation of the satellite-observed snow albedo ameliorates the simulation of upward shortwave radiation during the snow season, which is a prerequisite for an improved simulation of both the surface energy budget and the snowpack properties. These promising effects of snow albedo assimilation can help to reduce the uncertainties in the medium-range weather forecast as well as prediction of

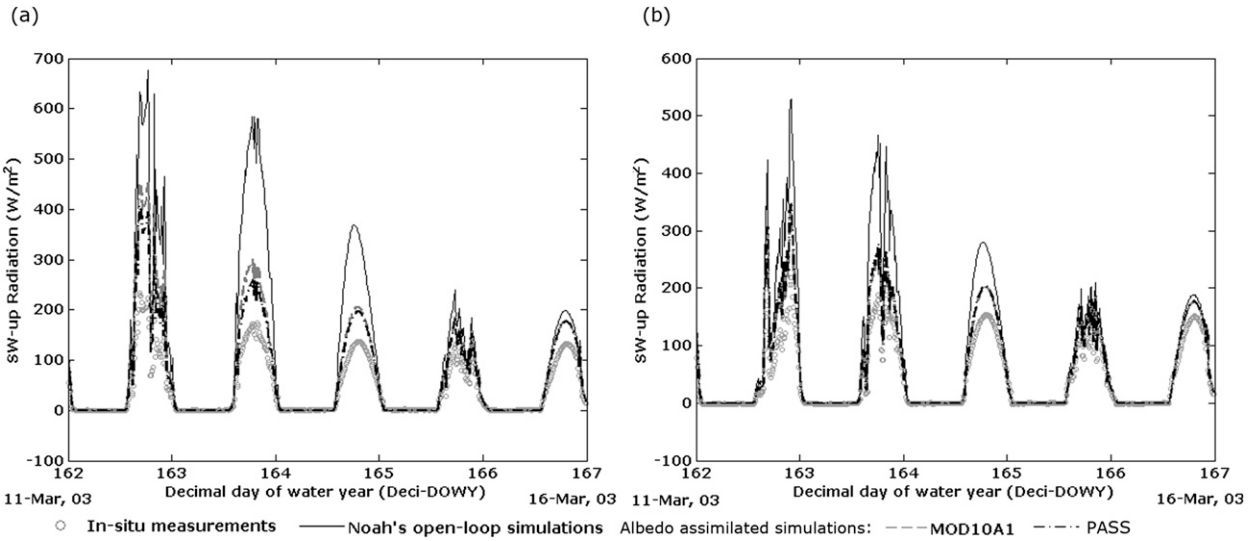

FIG. 9. Open-loop and updated Noah simulations for shortwave upward radiations along with the in situ measurements for (a) NM and (b) NP sites.

hydrological process (e.g., runoff). Further amelioration of the snow mass simulation is only possible with accurate knowledge of snow depth and/or water equivalent collected either via in situ measurement or from space. The data products that are expected to evolve from Earth Explorer missions of the European Space Agency (e.g., Cold Regions H_2O) and NASA (e.g., Snow and Cold Land Processes) can play an important role in this context.

Acknowledgments. This study was financially supported by the Higher Education Commission (HEC) of Pakistan and facilitated by NUFFIC (The Netherlands). We also would like to thank the Cold Land Processes Field Experiment (CLPX) team for the data collection and the National Snow and Ice Data Center (NSIDC) for making these datasets available. We acknowledge the contribution of two anonymous reviewers in improving the quality of the manuscript.

REFERENCES

Andreadis, K. M., and D. P. Lettenmaier, 2006: Assimilating remotely sensed snow observations into a macroscale hydrology model. *Adv. Water Resour.,* **29,** 872–886.

Barlage, M., and Coauthors, 2010: Noah land surface model modifications to improve snowpack prediction in the Colorado Rocky Mountains. *J. Geophys. Res.,* **115,** D22101, doi:10.1029/2009JD013470.

Cherkauer, K. A., L. C. Bowling, and D. P. Lettenmaier, 2003: Variable Infiltration Capacity cold land process model updates. *Global Planet. Change,* **38,** 151–159.

DeWalle, D. R., and A. Rango, 2008: *Principles of Snow Hydrology*. Cambridge University Press, 420 pp.

Ek, M. B., and Coauthors, 2011: North American Land Data Assimilation System Phase 2 (NLDAS-2): Development and applications. *GEWEX News,* No. 21, International GEWEX Project Office, Silver Spring, MD, 6–7.

——, and Coauthors, 2003: Implementation of Noah land surface model advances in the National Centers for Environmental Prediction operational mesoscale Eta model. *J. Geophys. Res.,* **108,** 8851, doi:10.1029/2002JD003296.

Elder, K., and A. Goodbody, 2004: CLPX-Ground: ISA main meteorological data. National Snow and Ice Data Center, Boulder, CO, digital media. [Available online at http://nsidc.org/data/docs/daac/nsidc0172_clpx_mainmet/.]

——, ——, D. Cline, P. Houser, G. E. Liston, L. Mahrt, and N. Rutter, 2009: NASA Cold Land Processes Experiment (CLPX 2002/03): Ground-based and near-surface meteorological observations. *J. Hydrometeor.,* **10,** 330–337.

Klein, A. G., and J. Stroeve, 2002: Development and validation of a snow albedo algorithm for the MODIS instrument. *Ann. Glaciol.,* **34,** 45–52.

Kokhanovsky, A. A., and E. P. Zege, 2004: Scattering optics of snow. *Appl. Opt.,* **43,** 1589–1602.

Liang, S., J. Stroeve, and J. E. Box, 2005: Mapping daily snow/ice shortwave broadband albedo from Moderate Resolution Imaging Spectroradiometer (MODIS): The improved direct retrieval algorithm and validation with Greenland in situ measurement. *J. Geophys. Res.,* **110,** D10109, doi:10.1029/2004JD005493.

Livneh, B., Y. Xia, K. E. Mitchell, M. B. Ek, and D. P. Lettenmaier, 2010: Noah LSM snow model diagnostics and enhancements. *J. Hydrometeor.,* **11,** 721–738.

Lyapustin, A., M. Tedesco, Y. Wang, T. Aoki, M. Hori, and A. Kokhanovsky, 2009: Retrieval of snow grain size over Greenland from MODIS. *Remote Sens. Environ.,* **113,** 1976–1987.

Malik, M. J., R. van der Velde, Z. Vekerdy, Z. Su, and M. F. Salman, 2011: Semi-empirical approach for estimating broadband albedo of snow. *Remote Sens. Environ.,* **115,** 2086–2095.

Mitchell, K. E., and Coauthors, cited 2005: The Community Noah Land-Surface Model (LSM): User's guide, public release version 2.7.1. [Available online at http://www.emc.ncep.noaa.gov/mmb/gcp/noahlsm/Noah_LSM_USERGUIDE_2.7.1.htm.]

Niu, G.-Y., and Coauthors, 2011: The community Noah land surface model with multiparameterization options (Noah-MP): 1. Model description and evaluation with local-scale measurements. *J. Geophys. Res.,* **116,** D12109, doi:10.1029/2010JD015139.

Painter, T. H., K. Rittger, C. McKenzie, P. Slaughter, R. E. Davis, and J. Dozier, 2009: Retrieval of subpixel snow covered area, grain size, and albedo from MODIS. *Remote Sens. Environ.,* **113,** 868–879.

Pan, M., and Coauthors, 2003: Snow process modeling in the North American Land Data Assimilation System (NLDAS): 2. Evaluation of model simulated snow water equivalent. *J. Geophys. Res.,* **108,** 8850, doi:10.1029/2003JD003994.

Rodell, M., and P. R. Houser, 2004: Updating a land surface model with MODIS-derived snow cover. *J. Hydrometeor.,* **5,** 1064–1075.

Salomonson, V. V., and I. Appel, 2004: Estimating fractional snow cover from MODIS using the normalized difference snow index. *Remote Sens. Environ.,* **89,** 351–360.

Stamnes, K., W. Li, H. Eide, T. Aoki, M. Hori, and R. Storvold, 2007: ADEOS-II/GLI snow/ice products—Part I: Scientific basis. *Remote Sens. Environ.,* **111,** 258–273.

Stroeve, J. C., J. E. Box, and T. Haran, 2006: Evaluation of the MODIS (MOD10A1) daily snow albedo product over the Greenland ice sheet. *Remote Sens. Environ.,* **105,** 155–171.

Sturm, M., J. Holmgren, and G. E. Liston, 1995: A seasonal snow cover classification system for local to global applications. *J. Climate,* **8,** 1261–1283.

Tedesco, M., and A. A. Kokhanovsky, 2007: The semi-analytical snow retrieval algorithm and its application to MODIS data. *Remote Sens. Environ.,* **111,** 228–241.

Wang, Z., X. Zeng, and M. Decker, 2010: Improving snow processes in the Noah land model. *J. Geophys. Res.,* **115,** D20108, doi:10.1029/2009JD013761.

Wigmosta, M. S., L. W. Vail, and D. P. Lettenmaier, 1994: A distributed hydrology-vegetation model for complex terrain. *Water Resour. Res.,* **30,** 1665–1679.

Wiscombe, W. J., and S. G. Warren, 1980: A model for the spectral albedo of snow. I: Pure snow. *J. Atmos. Sci.,* **37,** 2712–2733.

Xia, Y., M. Ek, H. Wei, and J. Meng, 2011: Comparative analysis of relationships between NLDAS-2 forcings and model outputs. *Hydrol. Processes,* **26,** 467–474, doi:10.1002/hyp.8240.

Zaitchik, B. F., and M. Rodell, 2009: Forward-looking assimilation of MODIS-derived snow-covered area into a land surface model. *J. Hydrometeor.,* **10,** 130–148.